
Interventional Sum-Product Networks: Causal Inference with Tractable Probabilistic Models

Matej Zečević
Computer Science Department,
TU Darmstadt
matej.zecevic@cs.tu-darmstadt.de

Devendra Singh Dhami
Computer Science Department,
TU Darmstadt
devendra.dhami@cs.tu-darmstadt.de

Athresh Karanam
Computer Science Department,
The University of Texas at Dallas
bvk180004@utdallas.edu

Sriraam Natarajan
Computer Science Department,
The University of Texas at Dallas
sriraam.natarajan@utdallas.edu

Kristian Kersting
Computer Science Department,
TU Darmstadt
kersting@cs.tu-darmstadt.de

Abstract

While probabilistic models are an important tool for studying causality, doing so suffers from the intractability of inference. As a step towards tractable causal models, we consider the problem of learning interventional distributions using sum-product networks (SPNs) that are over-parameterized by gate functions, e.g., neural networks. Providing an arbitrarily intervened causal graph as input, effectively subsuming Pearl’s *do*-operator, the gate function predicts the parameters of the SPN. The resulting *interventional* SPNs are motivated and illustrated by a structural causal model themed around personal health. Our empirical evaluation against competing methods from both generative and causal modelling demonstrates that interventional SPNs indeed are both expressive and causally adequate.

1 Introduction

Identifying causal relationships between variables in observational data is one of the fundamental and well-studied problem in machine learning. There have been several great strides in causality [Granger, 1969, Pearl, 2009, Bareinboim and Pearl, 2016] over the years specifically characterized by efforts that focused on reasoning about interventions [Hagmayer et al., 2007, Dasgupta et al., 2019] and counterfactuals [Morgan and Winship, 2015, Oberst and Sontag, 2019].

The notion of causality has long been explored in the realm of probabilistic models [Oaksford and Chater, 2017, Beckers and Halpern, 2019] with a special focus on graphical models, called causal Bayesian networks (CBNs) [Heckerman et al., 1995, Neapolitan, 2004, Pearl, 1995, Acharya et al., 2018]. CBNs have widely been applied to infer causal relationships in high-impact diverse applications such as disease progression [Koch et al., 2017], ecological risk assessment [Carriger and Barron, 2020] and more recently Covid-19 [Fenton et al., 2020, Feroze, 2020] to name a few. Although successful, classical CBN models are difficult to scale and also suffer from the problem of intractable inference. Recently, tractable probabilistic models such as probabilistic sentential decision diagrams [Kisa et al., 2014] and sum-product networks [Poon and Domingos, 2011] have emerged,

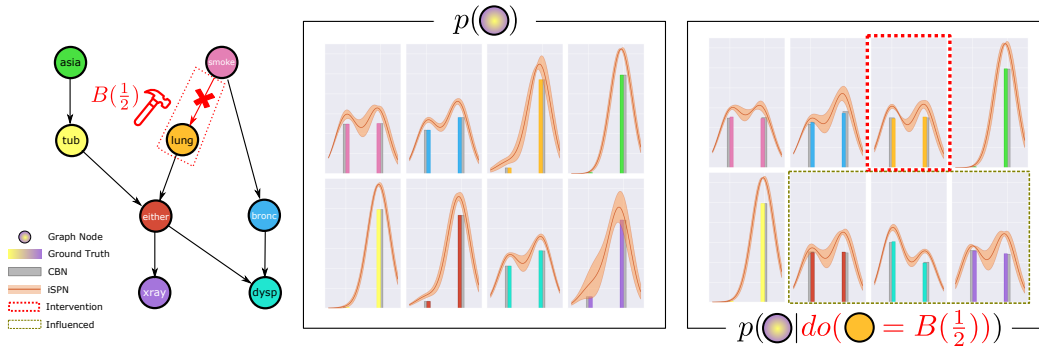


Figure 1: **Capturing interventional distributions using iSPN.** The interventional distributions for the ASIA data set using a causal Bayesian network (CBN, small-scale gold standard, gray bars) as well as an interventional SPN (iSPN) by intervening on *lung*. The iSPN is sensible to all the influences of the given intervention onto the system i.e., subsequent effects in the causal hierarchy. (Best viewed in color.)

which guarantee that conditional marginals can be computed in time linear in the size of the model. While weaving in the notion of interpretability, the computational view on probabilistic models allows one to exploit ideas from deep learning and can thus be very useful in modelling complex problems.

Recently, there has been an effort to take advantage of this tractability to reason for causality. Zhao et al. [2015] showed how to compile back and forth between sum-product networks (SPNs) and Bayesian networks (BNs). Although this opened up a whole range of possibilities for tractable causal models, Papantonis and Belle [2020] argued that such conversion leads to degenerated BNs thereby rendering it ineffective for causal reasoning. For the considered compilation of SPNs to BNs, this is indeed the case since a bipartite graph between the hidden and observed variables loses the relationships between the actual variables. Thus, either a new compilation method for transforming between tractable and causal model or alternatively a method to condition the probabilistic models directly on the *do*-operator to obtain interventional distributions, $P(y|do(x))$, is being required.

Here, we consider the latter strategy and extend the idea of conditionally parameterizing SPNs [Shao et al., 2019] by conditioning on the *do*-operator while predicting the complete set of observed variables therefore capturing the effect of intervention(s). The resulting *interventional sum-product networks (iSPNs)* take advantage of both the expressivity, due to the neural network, and the tractability, due to the SPN in order to capture the interventional distributions faithfully. This shows that the dream of tractable causal models is not insurmountable, since iSPNs are causal. Pearl [2019] defined a three-level causal hierarchy that separates association (purely statistical level 1) from intervention (level 2) and counterfactuals (level 3), and argued that the latter two levels involve causal inference. iSPNs are a modelling scheme for arbitrary interventional distributions. They just belong to level 2 and, in turn, are causal. So, while SPNs are not universal function approximators and the use of gate functions turns them into universal approximators, we go one step ahead and make the first effort towards introducing causality to SPNs without the need for compilation to Bayesian networks, as the functional approximator subsumes the *do*-operator. Fig. 1 shows an example of the effectiveness of iSPNs to capture interventional distributions on the ASIA data set. Our extensive experiments against strong baselines demonstrate that our method is able to capture ideal interventional distributions.

To summarize, we make the following contributions:

1. We introduce iSPNs, the first method that applies the idea of tractable probabilistic models to causality without the need for compilation and that accordingly generate interventional distributions w.r.t. the provided causal structure.
2. We formulate the inductive bias necessary for turning conditional SPN into iSPN while taking advantage of the neural network modelling capacities within the gating nodes for modelling interventional distributions while capturing all influences within the given intervention (i.e., consequences propagated through the structural hierarchy).
3. We show that by construction iSPNs can identify any interventional distribution permitted by the underlying structural causal model due to the inducted bias on the interface modalities in junction with the universal function approximation of the underlying gated SPN.

We proceed as follows. We start by reviewing the basic concepts required and related work. Then we introduce iSPNs and prove that by construction they are capable of approximating any *do*-query (given corresponding data). Before concluding, we present our experimental evaluation.

2 Background and Related Work

Let us briefly review the background on tractable probabilistic models and causal models used in subsequent sections for developing our new model class based on CSPNs that allow for identifying causal quantities i.e., interventional distributions.

Notation. We denote indices by lower-case letters, functions by the general form $g(\cdot)$, scalars or random variables interchangeably by upper-case letters, vectors, matrices and tensors with different boldface font \mathbf{v} , \mathbf{V} , \mathbf{V} respectively, and probabilities of a set of random variables \mathbf{X} as $p(\mathbf{X})$.

Sum-Product Networks (SPNs). Members of the family of probabilistic circuits [Van den Broeck et al., 2019] that satisfy certain properties such as decomposability and smoothness are known as sum-product networks¹. Introduced by Poon and Domingos [2011], SPNs represent a special type of probabilistic model that allows for a variety of exact and efficient inference routines. Generally, SPNs are considered as directed acyclic graphs (DAG) consisting of product, sum and leaf (or distribution) nodes whose structure and parameterization can be efficiently learned from data to allow for efficient modelling of joint probability distributions $p(\mathbf{X})$. Since their introduction, SPNs have been heavily studied such as by [Trapp et al., 2019] that present a way to learn SPNs in a Bayesian realm whereas [Kalra et al., 2018] learn SPNs in an online setting. Several different types of SPNs have also been studied such as Random SPN [Peharz et al., 2020b], Credal SPNs [Levray and Belle, 2020] and Sum-Product-Quotient Networks [Sharir and Shashua, 2018]) to name a few. For more details readers are referred to the survey of París, Sánchez-Cauce, and Díez [2020].

Gated SPNs. Conditional SPNs (CSPNs) are deep tractable models for estimating multivariate, conditional probability distributions $p(\mathbf{Y}|\mathbf{X})$ over mixed variables \mathbf{Y} [Shao et al., 2019]. They introduce functional gate nodes $g_i(\mathbf{X})$ that act as a functional parameterization of the SPN's information flow and leaf distributions given the provided evidence \mathbf{X} .

Causal Models. A Structural Causal Model (SCM) as defined by Peters et al. [2017] is specified as $\mathcal{C} := (\mathbf{S}, P_{\mathbf{N}})$ where $P_{\mathbf{N}}$ is a product distribution over noise variables and \mathbf{S} is defined to be a set of d structural equations

$$X_i := f_i(\text{pa}(X_i), N_i), \quad \text{where } i = 1, \dots, d \quad (1)$$

with $\text{pa}(X_i)$ representing the parents of X_i in graph $G(\mathcal{C})$. An intervention on a SCM \mathcal{C} as defined in (1) occurs when (multiple) structural equations are being replaced through new non-parametric functions $\hat{f}(\widehat{\text{pa}(X_i)}, \hat{N}_i)$ thus effectively creating an alternate SCM $\hat{\mathcal{C}}$. Interventions are referred to as *imperfect* if $\widehat{\text{pa}(X_i)} = \text{pa}(X_i)$ and as *atomic* if $\hat{f} = a$ for $a \in \mathbb{R}$. An important property of interventions often referred to as "modularity" or "autonomy"² states that interventions are fundamentally of local nature, formally

$$p^{\mathcal{C}}(X_i | \text{pa}(X_i)) = p^{\hat{\mathcal{C}}}(X_i | \text{pa}(X_i)), \quad (2)$$

where the intervention of $\hat{\mathcal{C}}$ occurred on variable X_k opposed to X_i . This suggests that mechanisms remain invariant to changes in other mechanisms which implies that only information about the effective changes induced by the intervention need to be compensated for. An important consequence of autonomy is the truncated factorization

$$p(V) = \prod_{i \notin S} p(X_i | \text{pa}(X_i)) \quad (3)$$

derived by Pearl [2009], which suggests that an intervention S introduces an independence of an intervened node X_i to its causal parents. Another important assumption in causality is that causal mechanisms do not change through intervention suggesting a notion of invariance to the cause-effect relations of variables which further implies an invariance to the origin of the mechanism i.e., whether it occurs naturally or through means of intervention [Pearl et al., 2016].

¹For decomposability and smoothness we refer to [Peharz et al., 2020a].

²See Section 6.6 in [Peters et al., 2017].

A SCM \mathcal{C} is capable of emitting various mathematical objects such as graph structure, statistical and causal quantities placing it at the heart of causal inference, rendering it applicable to machine learning applications in marketing [Hair Jr and Sarstedt, 2021]), healthcare [Bica et al., 2020]) and education [Hoiles and Schaar, 2016]. A SCM induces a causal graph G , an observational/associational distribution $p^{\mathcal{C}}$, can be intervened upon using the *do*-operator and thus generate interventional distributions $p^{\mathcal{C};do(\dots)}$ and given some observations \mathbf{v} can also be queried for interventions within a system with fixed noise terms amounting to counterfactual distributions $p^{\mathcal{C}|\mathbf{V}=\mathbf{v};do(\dots)}$. To query for samples of a given SCM, the structural equations are being simulated sequentially following the underlying causal structure starting from independent, exogenous variables and then moving along the causal hierarchy of endogenous variables (i.e., following the causal descendants).

The work closest to our work is by Brouillard et al. [2020] although it solves the different problem of causal discovery. Causality for machine learning has recently gained a lot of traction [Schölkopf, 2019] with the study of both interventions [Shanmugam et al., 2015] and counterfactuals [Kusner et al., 2017] gaining speed. For more details the readers are referred to [Zhang et al., 2018].

3 Interventional SPNs

Now we are ready to develop interventional SPNs (iSPNs). To this end, we re-introduce the importance of adaptability of models to interventional queries and present a newly curated synthetic data set to both motivate and validate the formalism of iSPNs that, through over-parametric extension of SPNs, allows them to adhere to causal quantities.

3.1 Adaptation to Causal Change

Peters et al. [2017] motivated the necessity of causality via the adequate generalizability of predictive models. Specifically, consider a simple regression problem $f(a) = b$ with data vectors $\mathbf{a}, \mathbf{b} \in \mathbb{R}^k$ that are strongly positively correlated in some given region, e.g. $(1 < a < \infty, 1 < b < \infty)$. Now a query is posed outside the data support, e.g. $(0, f(0))$. As argued by Peters et al., the underlying data generating processes can be an ambiguous causal process i.e., the data at hand can be explained by two different causal structures being either $A \rightarrow B$ or a common confounder with $A \leftarrow C \rightarrow B$.

Assuming the wrong causal structure or ignoring it altogether could be fatal, therefore, any form of generalization out of data support requires assumptions to be made about the underlying causal structure. We adopt this point of view and further argue that *ignoring causal change(s) in a system, i.e., the change of structural equation(s) underlying the system, can lead to a significant performance decrease and safety hazards*³. Therefore, it is important to account for distributional changes present in the data due to experimental (thus interventional) settings.

Consequently, we consider the learning problem, where the given data samples have been generated by different interventions $do(\mathbf{U}_j = \mathbf{u}_j)$ in a common SCM \mathcal{C} while the induced mutilated causal graphs $G(\mathcal{C}, do(\mathbf{U}_j = \mathbf{u}_j))$ are assumed to be known, such that the trained model is capable of at least inferring all involved causal distributions $p(V(\mathcal{C}) | do(\mathbf{U}_j = \mathbf{u}_j))$ with V being the variables.

3.2 Data Generating Process

To both validate and demonstrate the expressivity of interventional SPNs in modelling arbitrary interventional distributions, we curate a new causal data set based on the SCM \mathcal{C} presented in Fig. 2(a), which we subsequently refer to as *Causal Health* data set. The SCM encompasses four different structural equations of the form $V_i = f(\text{pa}(V_i), N_i)$, where $\text{pa}(V_i)$ are the parents of variable V_i and N_i are the respective noise terms that form a factor distribution $P^{N_{1:N}}$ i.e., the N_i are jointly independent. Now, the SCM \mathcal{C} describes the causal relations of an individual’s health and mobility attributes with respect to their age and nutrition.

Note that the Causal Health data set does not impose assumptions over the type of random variables or functional domains of the structural equations⁴, which additionally constraints a learned model to

³This extended notion of performance degeneration through ignorance to the underlying causality is prioritized in this paper.

⁴Assumptions on the func. form of structural eq. are crucial for identification (Tab. 7.1 [Peters et al., 2017])

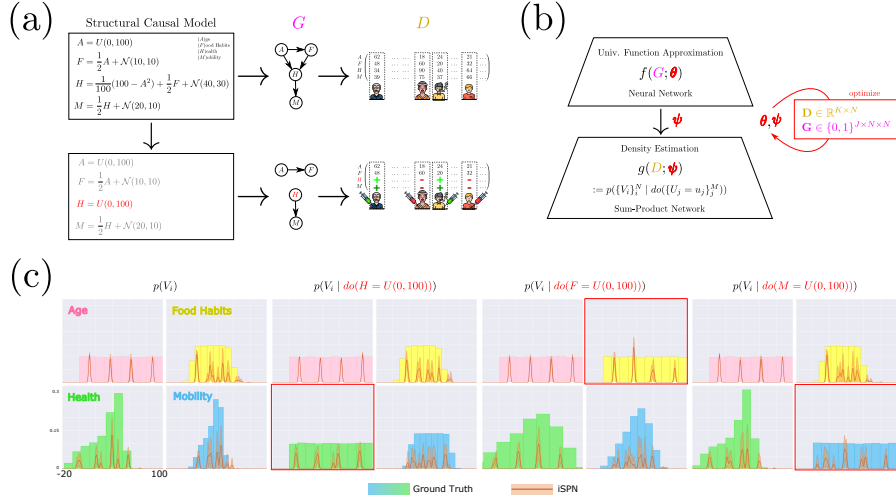


Figure 2: **An Overview of iSPN.** (a) The hidden process underlying the observable reality is modelled via a SCM that can be modified through interventions. The given SCM induces a causal graph and can generate data. An intervention can significantly alter the resulting data. (b) An over-parameterized density estimation framework using SPN is presented. The universal function approximator (here neural network) conditions on the mutilated causal graph and provides parameters to the SPN such that the given data’s density can be modelled accordingly. The FA subsumes the *do*-operator. (c) Different causal queries are being presented. Furthermore, iSPN adapts to intervention-consequences.

adapt flexibly. While we generally do not restrict our method to any particular type of intervention, the following mainly considers perfect interventions as introduced in Sec. 2.

Perfect interventions fully remove the causal mechanism of the parents of a given node, which is consistent with the idea behind that of randomized controlled trials (RCTs) where the given intervention randomizes the given specific node, often referred to as gold standard in causality related literature. We consider the special case of uniform randomization, i.e., uniform across the domain of the given variable⁵. An intervention performed on one node immediately changes the population and, thus, has a major effect on the generating processes of subsequent causal mechanisms in the respective causal sequence of events.

To provide the reader with a concrete example of interventions within the causal health data set, consider the following: In concern of a virus infection the individuals of the Causal Health study should be vaccinated. The vaccine is expected to have side-effect(s), however, it has been poorly designed and has reached the population with the capability of completely changing the individual’s health state. The observed changes do not show any form of pattern and are therefore assumed to be random. A young fit person could thus become sick, while an old person might feel better health wise. This sudden change will have an effect on the individual’s mobility and also be independent of their age and nutrition. Such a scenario is mathematically being captured through $do(H = U(H))$ where $U(\cdot)$ is the uniform distribution over a given domain.

3.3 Introducing Interventional SPNs

After motivating both the importance and the occurrences of interventions within relevant systems, we now start introducing interventional SPNs (iSPNs).

Definition of iSPN. As motivated in Sec. 1, the usage of the compilation method from [Zhao et al., 2015] for causal inference within SPN is arguably of degenerate⁶ nature given the properties of the compilation method [Papantonis and Belle, 2020]. While the results of Papantonis and Belle [2020] are arguably negative, there exists *yet no proof of non-existence of such a compilation method* and as the authors point out in their argument for future lines of research in this direction, a model class extension poses a viable candidate for overcoming the problems of using SPN for causal inference.

⁵Note that for binary variables this amounts to Bernoulli $B(\frac{1}{2})$.

⁶A bipartite graph in which the actual variables of interest are not connected is called degenerate.

While agreeing on the latter aspect, we do not go the “compilation road” but extend the idea of conditional parameterization for SPN [Shao et al., 2019] by conditioning on a modified form of the *do*-operator introduced by Pearl [2009] while predicting the complete set of observed variables.

Mathematically, we estimate $p(V_i | do(\mathbf{U}_j = \mathbf{u}_j))$ by learning a non-parametric function approximator $f(\mathbf{G}; \boldsymbol{\theta})$ (e.g. neural network), which takes as input the (mutilated) causal graph $\mathbf{G} \in \{0, 1\}^{N \times N}$ encoded as an adjacency matrix, to predict the parameters $\boldsymbol{\psi}$ of a SPN $g(\mathbf{D}; \boldsymbol{\psi})$ that estimates the density of the given data matrix $\{\mathbf{V}_k\}_k^K = \mathbf{D} \in \mathbb{R}^{K \times N}$. With this, iSPNs are defined as follows:

Definition 1 (Interventional Sum-Product Network). *An interventional sum-product network (iSPN) is the joint model $m(\mathbf{G}, \mathbf{D}) = g(\mathbf{D}; \boldsymbol{\psi} = f(\mathbf{G}; \boldsymbol{\theta}))$, where $g(\cdot)$ is a SPN, $f(\cdot)$ a non-parametric function approximator and $\boldsymbol{\psi} = f(\mathbf{G})$ are shared parameters.*

They are called interventional because we consider it to be a causal model given its capability of answering queries from the second level of the causal hierarchy [Pearl, 2019], namely, that of interventions⁷. The shared parameters $\boldsymbol{\psi}$ allow for information flow during learning between the conditions and the estimated densities. Setting the conditions such that they contain information about the interventions, in the form of the mutilated graphs \mathbf{G} , effectively renders f to subsume a sort of *do*-calculus in the spirit of truncated factorization shown in Eq.(3) i.e., the gate model acts as an estimator selector. Generally, we note that our formulation allows for different function and density estimators f, g . We choose f to be a neural network for two reasons (1) their empirically established capability to act as causal sub-modules (e.g. Ke et al. [2019] use a cohort of neural nets to mimic a set of structural equations, thus, a SCM) and (2) their model capacity being a universal function approximator, while we choose g to be a SPN for its tractability properties for inference.

We have argued the importance of adaptability to interventional changes within the causal system and intend now to prove that iSPN are capable of approximating these different causal quantities.

Proposition 1 (Expressivity). *Assuming autonomy and invariance, an iSPN $m(\mathbf{G}, \mathbf{D})$ is able to identify any interventional distribution $p_G(\mathbf{V}_i = \mathbf{v}_i | do(\mathbf{U}_j = \mathbf{u}_j))$, permitted by a SCM \mathcal{C} through interventions, with knowledge of the mutilated causal graph $\hat{\mathbf{G}}$ and data \mathbf{D} generated from the intervened SCMs by modelling the conditional distribution $p_{\hat{\mathbf{G}}}(\mathbf{V}_i = \mathbf{v}_i | \mathbf{U}_j = \mathbf{u}_j)$.*

Proof. It follows directly from the definition of the *do*-calculus [Pearl, 2009] that $p_G(\mathbf{V}_i = \mathbf{v}_i | do(\mathbf{U}_j = \mathbf{u}_j)) = p_{\hat{\mathbf{G}}}(\mathbf{V}_i = \mathbf{v}_i | \mathbf{U}_j = \mathbf{u}_j)$ where $\hat{\mathbf{G}}$ is the mutilated causal graph according to the intervention $do(\mathbf{U}_j = \mathbf{u}_j)$ i.e., observations in the intervened system are akin to observations made when intervening on the system. Given the mutilated causal graph $\hat{\mathbf{G}}$ (as adjacency matrix), the only remaining aspect to show is that the density estimating SPN can approximate a joint probability $p(\mathbf{X})$ using \mathbf{D} . This naturally follows from [Poon and Domingos, 2011]. \square

The expressivity of iSPN stems from both the capacities of gate function and the knowledge of intervention as well as availability of respective data. As an important remark, causal inference is often interested in estimating interventional distributions, i.e, causal quantities from purely observational models. Therefore, an alternative formulation to Prop. 1 would be to replace the knowledge of the intervened causal structure \mathbf{G} with knowledge on a valid adjustment set. In the following, we only consider the direct setting where actual interventional data from the system is assumed to be captured⁸ thereby freeing the investigation of iSPN from the independent research around hidden confounding.

Universal Function Approximation (UFA). The gating nodes of CSPNs extend SPNs in a way that allows them to also induce functions which are universal approximators. For instance, using threshold gates $x_i \leq c \in \mathbb{R}$, one can realize testing arithmetic circuits [Choi and Darwiche, 2018] which have been proven to be universal approximators - rendering iSPN to be UFA by construction.

Learning of iSPN. An interventional sum-product network is being learned using a set of mixed-distribution samples generated from simulating the Causal Health SCM for different interventions, where the observational case is considered to be equivalent to an intervention on the empty set. The parameters $\boldsymbol{\theta}, \boldsymbol{\psi}$ of the iSPN describe the weights of the gate nodes and the distributions at the leaf nodes. The full model m is differentiable if the provided gate function f and each of the leaf models of g are differentiable. Therefore, to train an iSPN, as depicted in Fig. 2(b), it is sufficient to optimize

⁷The first level of the causal hierarchy —association— is considered to be purely statistical.

⁸For details on the remarked alternative formulation consider the Supplement.

the conditional log-likelihood end-to-end using gradient based optimization techniques. We assess the performance of our learned model through inspection of the adaptation of the model to the different interventions manifesting in the resulting marginals $p(V_i | do(U_j))$.

As can be observed in Fig. 2(c) or alternatively in Fig. 4 (top row), the learned iSPN successfully adapts to both the interventions as well as its consequences. Considering for instance the intervention $p(V_i | do(F = B(\frac{1}{2})))$ which removes the edge $A \rightarrow F$ and thus renders Age (A) and Food Habits (F) independent. Given the drastic population change in F and the fact that the Health (H) of an individual is causally dependent on both A and F a significant change in H is being expected. Indeed, both H and Mobility (M), being a causal child of H , broaden distribution wise and also these subsequent changes are captured correctly.

Discussion. To reconsider and answer the general question of why the modelling of a conditional distribution via an over-parameterized architecture is a sensible idea consider the following. One can represent a conditional distribution $p(\mathbf{Y} | \mathbf{X})$ by applying Bayes Rule to a joint distribution density model (e.g. a regular SPN) $p(\mathbf{Y} | \mathbf{X}) = \frac{p(\mathbf{Y}, \mathbf{X})}{p(\mathbf{X})}$. However, this assumes non-empty support i.e., $p(\mathbf{X}) > 0$. Furthermore, the joint distribution $p(\mathbf{Y}, \mathbf{X})$ optimizes *all* possibly derivable distributions, diminishing single distr. expressivity. Therefore, our considered formulation of a gate model allows for effectively subsuming the *do*-operator i.e., the gate model orchestrates the *do* queries such that the density estimator can easily switch between different interventional distributions. While not introducing specific limitations, general CSPN limitation regarding OOD generalization are inherited.

Method \ Query	V_1	V_2	V_3	V_4
iSPN	.001 ± .00	.007 ± .01	.003 ± .00	.013 ± .01
MADE	.588 ± .59	.108 ± .16	.015 ± .02	.105 ± .12
MDN	.178 ± .14	.263 ± .14	.184 ± .12	.079 ± .01

Table 1: **Jensen-Shannon-Divergence Evaluation of Estimated Interventional Distributions.** Numerical pendant to Fig.4, mean and standard deviation per $p(V_{j \setminus i} | do(V_i = U(V_i)))$ where U is the uniform distribution across all data sets. Lower is better.

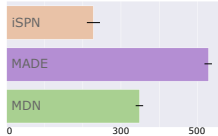


Figure 3: **Mean Running Times in sec. till convergence (Causal Health)** for 50 full passes. More data sets results in supplementary.

4 Experimental Results

The assumptions made in causality usually require control over the data generating process which is almost never readily available in the real world. This amounts to scarcity of the available public data sets and also their implications for transfers to the real world and even when available, they are usually artificially generated as some causal extension of a known, pre-existing data set (e.g. MorphoMNIST data set introduced by Castro et al. [2019]). While it is difficult to consider real-world-esque experimental settings for causal models, we do not restrict our investigations of iSPN to rather specific problem settings like certain noise or decision variable instances (which is common in causal inference). The evaluation is performed on data sets with varying number of variables and in both continuous and discrete domains. For the introduced causal health data set, we even consider arbitrary underlying noise distributions. We have made our code repository publicly available⁹.

Data Sets. We evaluate iSPNs on four data sets. Three benchmarks: ASIA (A) [Lauritzen and Spiegelhalter, 1988] with 8 variables, Earthquake (E) with 5 variables and Cancer (C) [Korb and Nicholson, 2010] with 5 variables. One newly curated synthetic causal health (H) data set with 4 variables. More information about the data sets is presented in the Supplement.

Baselines. For *generative* capacities, we compare our method against Mixture Density Networks (MDN) [Bishop, 1994] and Masked Autoencoder for Density Estimation (MADE) [Germain et al., 2015]. Both methods are expressive, parametric neural network based approaches for density estimation. Generally, the causality for machine learning literature suggests a strong favor for neural based function approximators for modelling causal mechanisms [Ke et al., 2019]. For *causal* capacities, we compare our method against the renown causal baselines from CausalML [Chen et al., 2020] and DoWhy [Sharma and Kiciman, 2020] for the modelling of average treatment effects (ATE) [Pearl, 2009, Peters et al., 2017] considered to be a gold standard task within causal inference.

⁹<https://anonymous.4open.science/r/8a12a810-3343-4950-a5de-bd0721f4e914/>

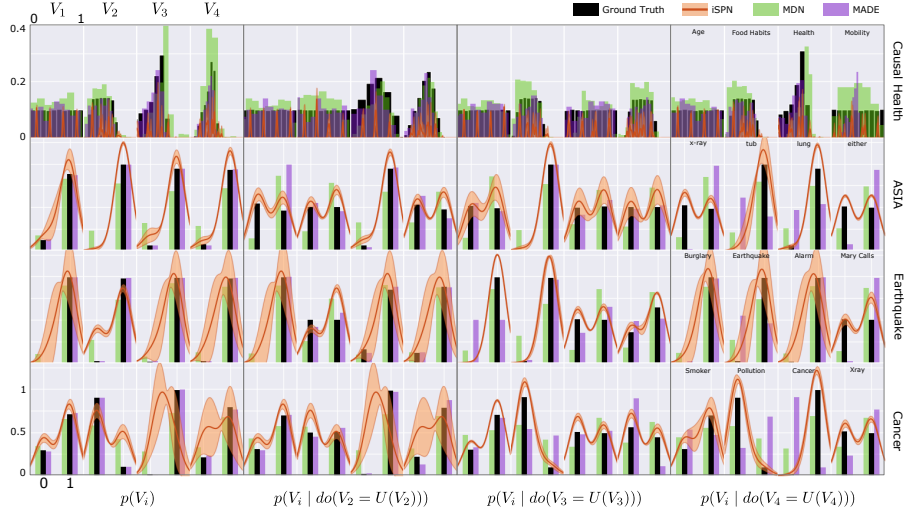


Figure 4: **Generative Baselines.** A comparison to the ground-truth (via underlying SCM) and competing estimated distributions. Each row represents a data set and each column represents a variable for a given causal query. (Best in color.)

Protocol and Parameters. To account for reproducibility and stability of the presented results, we used learned models for five different random seeds per configuration. For means of visual clarity, the competing baselines MDN and MADE only present the best performing seed while iSPN is being presented with a mean plot and the standard deviation. The CBN, which performs exact inference according to the *do*-calculus (while best performing) has to be considered as gold standard and is therefore not part of the visualization. Furthermore, as it cannot compare in terms of feasibility. The considered interventions were of uniform nature. Each block of four columns represents a variable being randomized uniformly. We deployed a RAT-SPN [Peharz et al., 2020b] selecting the leaf node distributions to be Gaussian distributions. For further experimental details consider the Supplement.

Our empirical analysis investigates iSPN for the following questions: **Q1:** How is the estimation quality for interv. distributions? **Q2:** How important is the model’s capacity? **Q3/4:** How is the performance relative to S.o.t.A. generative and causal models? **Q5:** How is the runtime performance?

(Q1. Precise Estimation of *do*-influenced variables) The density functions learned by iSPN (see Fig. 4) fit with a high degree of precision as visualized by the difference in the peak of the modes of the learned distribution and that of the ground truth. While our visual analysis is arguably the superior method of evaluation as it conveys information about how the distributions of interest compare (which is feasible due to marginal inference and the locality of interventions within a SCM), we have also considered numerical evaluation criteria like the Jensen-Shannon-Divergence on which (as visually confirmed) iSPN outperforms the baselines (see Tab.1). For more detailed observation and interpretation consider the Supplement.

(Q2. Capacity Ablation Study) We test the robustness of iSPN as the size of the associated SPN $g(\mathbf{D}; \psi)$ is varied. We obtain 5 different iSPNs for each of the 4 data sets by using 5 different numbers of sum node weights, 600, 1200, 1800, 2400, 3200, effectively changing the capacity of the parameter-sharing neural network $f(\mathbf{G}; \theta)$. We observe iSPNs to be robust to varying hyperparameters that control the size of the SPN $g(\cdot)$ and effectively the complexity of the associated function approximator $f(\cdot)$. More details and figures are in the Supplement.

(Q3. Comparison to Generative models) We compare the performances in terms of precision of fit of the learned distributions as well as the flexibility of the models. iSPN outperforms the baselines across all 4 data sets both in precision of the fit of the learned density functions and flexibility of adaptation to the different interventions as seen in figure 4. In our experiments, MDN had the worst performance with estimated densities being consistently and significantly different from the ground truth, as the model settled for an average distribution across all interventions. MADE is able to estimate to high precisions but showed to be generally inconsistent across the experimental settings.

(Q4. Comparison to Causal models) We compare the numerical results as seen in figure 5 and observe that iSPN matches the performance of the causal baselines. The simple regressor employed

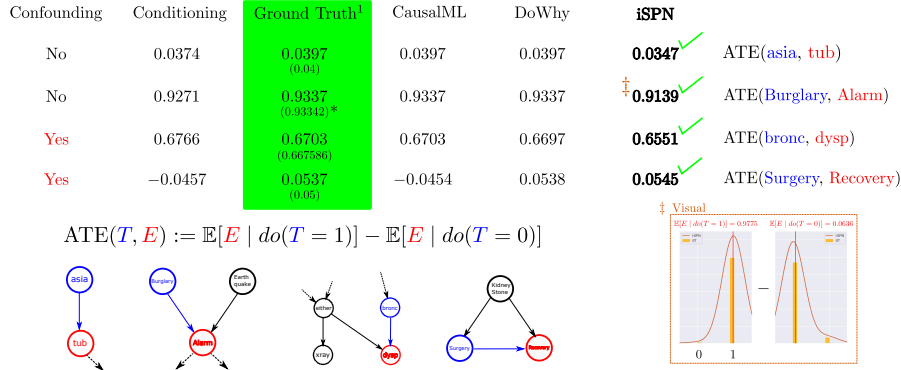


Figure 5: **Causal Baselines.** Different causal structures and corresponding causal effect estimation methods (CausalML, DoWhy) are being compared against iSPN. When confounding is present, then conditioning becomes different from intervening $p(Y \mid X) \neq p(Y \mid do(X))$ and iSPN correctly captures all evaluated cases. (* are analytical solutions, ¹ differences of means for actual interventional distributions, Best viewed in color.)

by CausalML fails in the confounding case as it estimates wrongly the conditional, both DoWhy and iSPN can handle even the more difficult Simpson’s paradox [Simpson, 1951] scenario. An analytical derivation for the ATE is exemplified in the Supplement.

(Q5. Comparison of running times) SPNs are tractable by design as long the networks size is polynomial in the input size. The superiority in running time also becomes apparent during training on the same (Causal Health) data set where we observe the mean run times over 50 passes of the whole data set to be significantly faster than competing methods (see Fig.3).

5 Conclusions

We presented a way to connect causality with tractable probabilistic models by using sum-product networks parameterized by universal function approximators in the form of neural networks. We show that our proposed method can adapt to the underlying causal changes in a given domain and generate near perfect interventional distributions irrespective of the data distribution and the intervention type thereby exhibiting flexibility. Our empirical evaluation shows that our method is able to precisely estimate the conditioned variables and outperform generative baselines.

Finding a different compilation method for SPNs such as by making use of tree CBNs is important for learning pure causal probabilistic models. Testing our method on larger real world causal data sets is an interesting direction. Finally, using rich expert domain knowledge in addition to observational data is essential for causality and extending our method to incorporate such knowledge is essential.

References

- Jayadev Acharya, Arnab Bhattacharyya, Constantinos Daskalakis, and Saravanan Kandasamy. Learning and testing causal models with interventions. *NeurIPS*, 2018.
- Elias Bareinboim and Judea Pearl. Causal inference and the data-fusion problem. *PNAS*, 2016.
- Sander Beckers and Joseph Y Halpern. Abstracting causal models. In *AAAI*, 2019.
- Ioana Bica, Ahmed Alaa, and Mihaela Van Der Schaar. Time series deconfounder: Estimating treatment effects over time in the presence of hidden confounders. In *ICML*, 2020.
- Christopher M Bishop. Mixture density networks. 1994.
- Philippe Brouillard, Sébastien Lachapelle, Alexandre Lacoste, Simon Lacoste-Julien, and Alexandre Drouin. Differentiable causal discovery from interventional data. *NeurIPS*, 2020.
- John F Carriger and Mace G Barron. A bayesian network approach to refining ecological risk assessments: Mercury and the florida panther (*puma concolor coryi*). *Ecological Modelling*, 2020.
- Daniel C Castro, Jeremy Tan, Bernhard Kainz, Ender Konukoglu, and Ben Glocker. Morpho-mnist: quantitative assessment and diagnostics for representation learning. *Journal of Machine Learning Research*, 20(178):1–29, 2019.
- Huigang Chen, Totte Harinen, Jeong-Yoon Lee, Mike Yung, and Zhenyu Zhao. Causalml: Python package for causal machine learning. *arXiv preprint arXiv:2002.11631*, 2020.
- Arthur Choi and Adnan Darwiche. On the relative expressiveness of bayesian and neural networks. In *International Conference on Probabilistic Graphical Models*, pages 157–168. PMLR, 2018.
- Ishita Dasgupta, Jane Wang, Silvia Chiappa, Jovana Mitrovic, Pedro Ortega, David Raposo, Edward Hughes, Peter Battaglia, Matthew Botvinick, and Zeb Kurth-Nelson. Causal reasoning from meta-reinforcement learning. *arXiv preprint arXiv:1901.08162*, 2019.
- Norman E Fenton, Martin Neil, Magda Osman, and Scott McLachlan. Covid-19 infection and death rates: the need to incorporate causal explanations for the data and avoid bias in testing. *Journal of Risk Research*, 2020.
- Navid Feroze. Forecasting the patterns of covid-19 and causal impacts of lockdown in top five affected countries using bayesian structural time series models. *Chaos, Solitons & Fractals*, 2020.
- Mathieu Germain, Karol Gregor, Iain Murray, and Hugo Larochelle. Made: Masked autoencoder for distribution estimation. In *International Conference on Machine Learning*, pages 881–889. PMLR, 2015.
- Clive WJ Granger. Investigating causal relations by econometric models and cross-spectral methods. *Econometrica: journal of the Econometric Society*, 1969.
- York Hagmayer, Steven A Sloman, David A Lagnado, and Michael R Waldmann. Causal reasoning through intervention. *Causal learning: Psychology, philosophy, and computation*, 2007.
- Joseph F Hair Jr and Marko Sarstedt. Data, measurement, and causal inferences in machine learning: opportunities and challenges for marketing. *Journal of Marketing Theory and Practice*, 2021.
- David Heckerman, Dan Geiger, and David M Chickering. Learning bayesian networks: The combination of knowledge and statistical data. *Machine learning*, 1995.
- William Hoiles and Mihaela Schaar. Bounded off-policy evaluation with missing data for course recommendation and curriculum design. In *ICML*, 2016.
- Agastya Kalra, Abdullah Rashwan, Wei-Shou Hsu, Pascal Poupart, Prashant Doshi, and Georgios Trimonias. Online structure learning for feed-forward and recurrent sum-product networks. *NeurIPS*, 2018.

- Nan Rosemary Ke, Olexa Bilaniuk, Anirudh Goyal, Stefan Bauer, Hugo Larochelle, Bernhard Schölkopf, Michael C Mozer, Chris Pal, and Yoshua Bengio. Learning neural causal models from unknown interventions. *arXiv preprint arXiv:1910.01075*, 2019.
- Doga Kisa, Guy Van den Broeck, Arthur Choi, and Adnan Darwiche. Probabilistic sentential decision diagrams. In *KR*, 2014.
- Daniel Koch, Robert S Eisinger, and Alexander Gebharter. A causal bayesian network model of disease progression mechanisms in chronic myeloid leukemia. *Journal of theoretical biology*, 2017.
- Kevin B Korb and Ann E Nicholson. *Bayesian artificial intelligence*. CRC press, 2010.
- Matt J Kusner, Joshua R Loftus, Chris Russell, and Ricardo Silva. Counterfactual fairness. *NeurIPS*, 2017.
- Steffen L Lauritzen and David J Spiegelhalter. Local computations with probabilities on graphical structures and their application to expert systems. *Journal of the Royal Statistical Society: Series B (Methodological)*, 1988.
- Amélie Levray and Vaishak Belle. Learning credal sum-product networks. *AKBC*, 2020.
- Stephen L Morgan and Christopher Winship. *Counterfactuals and causal inference*. Cambridge University Press, 2015.
- Richard E. Neapolitan. *Learning bayesian networks*. Pearson Prentice Hall Upper Saddle River, NJ, 2004.
- Mike Oaksford and Nick Chater. Causal models and conditional reasoning. *Oxford library of psychology. The Oxford handbook of causal reasoning*, 2017.
- Michael Oberst and David Sontag. Counterfactual off-policy evaluation with gumbel-max structural causal models. In *ICML*, 2019.
- Ioannis Papantonis and Vaishak Belle. Interventions and counterfactuals in tractable probabilistic models: Limitations of contemporary transformations. *arXiv preprint arXiv:2001.10905*, 2020.
- Iago París, Raquel Sánchez-Cauce, and Francisco Javier Díez. Sum-product networks: A survey. *arXiv preprint arXiv:2004.01167*, 2020.
- Judea Pearl. From bayesian networks to causal networks. In *Mathematical models for handling partial knowledge in artificial intelligence*. 1995.
- Judea Pearl. *Causality*. Cambridge university press, 2009.
- Judea Pearl. The seven tools of causal inference, with reflections on machine learning. *Communications of the ACM*, 62(3):54–60, 2019.
- Judea Pearl, Madelyn Glymour, and Nicholas P Jewell. *Causal inference in statistics: A primer*. John Wiley & Sons, 2016.
- Robert Peharz, Steven Lang, Antonio Vergari, Karl Stelzner, Alejandro Molina, Martin Trapp, Guy Van den Broeck, Kristian Kersting, and Zoubin Ghahramani. Einsum networks: Fast and scalable learning of tractable probabilistic circuits. *ICML*, 2020a.
- Robert Peharz, Antonio Vergari, Karl Stelzner, Alejandro Molina, Xiaoting Shao, Martin Trapp, Kristian Kersting, and Zoubin Ghahramani. Random sum-product networks: A simple and effective approach to probabilistic deep learning. In *UAI*, 2020b.
- Jonas Peters, Dominik Janzing, and Bernhard Schölkopf. *Elements of causal inference*. The MIT Press, 2017.
- Hoifung Poon and Pedro Domingos. Sum-product networks: A new deep architecture. In *2011 IEEE International Conference on Computer Vision Workshops (ICCV Workshops)*, pages 689–690. IEEE, 2011.

- Bernhard Schölkopf. Causality for machine learning. *arXiv preprint arXiv:1911.10500*, 2019.
- Karthikeyan Shanmugam, Murat Kocaoglu, Alexandros G Dimakis, and Sriram Vishwanath. Learning causal graphs with small interventions. *NeurIPS*, 2015.
- Xiaoting Shao, Alejandro Molina, Antonio Vergari, Karl Stelzner, Robert Peharz, Thomas Liebig, and Kristian Kersting. Conditional sum-product networks: Imposing structure on deep probabilistic architectures. *arXiv preprint arXiv:1905.08550*, 2019.
- Or Sharir and Amnon Shashua. Sum-product-quotient networks. In *AISTATS*, 2018.
- Amit Sharma and Emre Kiciman. Dowhy: An end-to-end library for causal inference. *arXiv preprint arXiv:2011.04216*, 2020.
- Edward H Simpson. The interpretation of interaction in contingency tables. *Journal of the Royal Statistical Society: Series B (Methodological)*, 13(2):238–241, 1951.
- Martin Trapp, Robert Peharz, Hong Ge, Franz Pernkopf, and Zoubin Ghahramani. Bayesian learning of sum-product networks. *NeurIPS*, 2019.
- G Van den Broeck, N Di Mauro, and A Vergari. Tractable probabilistic models: Representations, algorithms, learning, and applications. *Tutorial at UAI*, 2019.
- Kun Zhang, Bernhard Schölkopf, Peter Spirtes, and Clark Glymour. Learning causality and causality-related learning: some recent progress. *National science review*, 2018.
- Han Zhao, Mazen Melibari, and Pascal Poupart. On the relationship between sum-product networks and bayesian networks. In *ICML*, 2015.

A Appendix

We make further use of this supplementary section following the main paper to introduce some additional insights and results we deem important for the reader and for what has been examined in the main paper.

A.1 Ablation Study on Arbitrary Intervention Realizations

In the main paper we have mostly considered perfect interventions i.e., interventions that render the intervened variables and its causal parents independent, and especially uniformly randomization as interventions which are consistent in their nature with the idea behind RCTs that are often argued to be the gold standard in causality. However, as already suggested, our model is not restricted to any specific intervention type or instantiation. Fig. 6 (a) illustrates the performance of iSPN on the Causal Health data set for different intervention types (perfect, atomic), noise terms (Gaussian, Gamma, Beta) and instantiations (Indicator Functions, Modifications). As can be observed, the model successfully manages to model most interventional distributions and consequences adequately. Furthermore, we observe that the training curves remained consistent among different intervention types further advocating the adaptability of the model to interventions of more arbitrary nature. Nonetheless, it can be observed that some interventions are being modelled more precisely than others, e.g. consider the relatively better performance of the model on the non-standard Beta intervention $do(H = 100B(2, 2))$ that creates a wide and symmetric distribution opposed to the indicator intervention $do(H = 1_{[25, 75]})$ that creates two heaps on 25 and 75. A possible explanation for this observation might lie in the fact that the model still learns other variants of distributions for a given variable, i.e. the different distributions the model adapts to on e.g. the Health H variable are $p(H), p(H | do(F = f)), p(H | do(M = m))$ etc. and it can be argued that the non-standard Beta intervention is more consistent (that is, more similar) with these other marginal distributions of H than it is with the unconventional distribution it learns for the indicator intervention. To summarize, the optimization problem becomes easier for the former.

A.2 On the Visualization of Mean Densities

Another notable aspect for further informing the results from the main paper is to note that the visualization scheme, used in the main paper for assessing a given models performance, always considers learned models under multiple random seeds (i.e., their mean and standard deviation density functions) and never for a given single best seed. The natural motivation for the usage of multiple random seeds is to account for robustness and reproducibility within the results, however, a single best seed can significantly outperform the respective mean performance of a configuration, especially in regions of low data support which is not directly observable in the visualizations. Therefore, in Fig. 7 we show an example for the atomic intervention $do(H = 50)$. It can be observed that the single best seed fits the given ground truth perfectly without compromising for other learned distributions which does not become directly evident by observing the plotted mean performance. We argue that this is an important consideration to have in mind during visual inspection for adequate assessment of the observed results.

A.3 Ablation Study on Function Approximator Capacity

As within the main paper, we perform an ablation study on the consequences of increasing or decreasing the function approximator (neural network) capacity for training any given configuration of iSPN. Fig. 10 visualizes the results for the remaining data sets not covered within the main paper i.e. Earthquake, Cancer and Causal Health. For Earthquake and Cancer data sets, we use 5 different number of sum node weights: 600, 1200, 1800, 2400 and 3200. For the synthetic causal health data set we use 300, 600, 1000, 1500, 2000. Each iSPN trained using these parameters is initialized over 5 random seeds. These values were chosen to test the performance of iSPN as they are increased/decreased compared to the optimal values of 2400 (600) for the public (synthetic) data sets. Interestingly, higher variances too, as seen in $p(V_3 | do(V_1 = U(V_1)))$, with V_3 being Xray and V_1 being Dyspnoea respectively, in the Cancer data set, are consistent across the 5 different iSPNs. The results are overall consistent with the presented i.e., the mean performance are consistent across the different neural network sizes while the variance can vary slightly on the presented data sets.

A.4 Data sets for Generative and Causal Inference Tasks

Additional details on the four data sets considered for empirical evaluation of the generative and causal capabilities of iSPN in comparison to SotA methods:

Data	# of variables	# of samples	# of edges
Causal Health	4	100,000	4
ASIA	8	10,000	8
Earthquake	5	10,000	4
Cancer	5	10,000	4

Table 2: **Dimensions of the used data sets.** Edges refer to the edges in the causal graph associated with each data set. The benchmarks stem from: <https://www.bnlearn.com/bnrepository/discrete-small.html>

A.5 Additional Experimental Details, Observation and Interpretation

Legend for Figure 4, data sets from top to bottom: H,A, E, C, variables from left to right: H: Age, Food Habits, Health, Mobility; A: Xray, Tub, Lung, Either; E: Burg., Earth., Alarm; C: Smoker, Poll., Cancer, Xray. We trained iSPNs on 10,000 samples for each of the 3 public data sets and on 100,000 samples for the synthetic Causal Health data set. We chose the non-parametric function approximators $f(\cdot)$ for each iSPN to be a multi-layer perceptron (MLP). The inputs to the MLPs were mutilated causal graphs \hat{G} . The MLPs had 2 hidden layers consisting of 10 units each and used ReLU as their activation functions. The outputs were 2400 (600) weights corresponding to the sum nodes and 96 (12) weights corresponding to the leaf nodes of the SPN $g(\mathbf{D}; \psi)$ for ASIA, Cancer and Earthquake (Causal Health) data sets. The MLPs were trained for 20 (130) epochs with a batch size of 100 (1000) and 5 different seeds.

Also, the learned distributions are similar across different seeds, with exception of some distributions, such as the marginal $p(V_4 | do(V_2 = U(V_2)))$ in the Cancer data set. A possible explanation for the observed higher variance is that the optimization trajectories during training for the different random seeds deviate with similar variance, stemming from the fact that different seeds select different initializations of the neural network parameters θ leading to different optimization steps and possibly local optima. A hint to this deviation of optimization trajectories might also be the observed discrepancy between the single best seed of a given model configuration and its mean performance across multiple random seeds as is being pointed out to the reader in the Appendix A.2.

All of the experiments have been conducted on a MacBook Pro (13-inch, 2020, Four Thunderbolt 3 ports) laptop running a 2,3 GHz Quad-Core Intel Core i7 CPU with a 16 GB 3733 MHz LPDDR4X RAM on time scales ranging from seconds to (a few) hours with increasing size of the experiments.

A.6 Alternative Formulation with an Adjustment Set

The following is an alternative to Prop.1 such that one exchanges the necessity of intervention with the knowledge on confounders if available.

Proposition 2 (Adjustment for Observational Models). *Assuming autonomy and invariance, any interventional distribution $p_G(\mathbf{V}_i = \mathbf{v}_i | do(\mathbf{U}_j = \mathbf{u}_j))$ permitted by a SCM \mathcal{C} that induces a causal graph G can be identified by adjusting for the confounders \mathbf{w} within the observational model $\sum_{\mathbf{w}} p(\mathbf{V}_i = \mathbf{v}_i | \mathbf{U}_j = \mathbf{u}_j, \mathbf{W} = \mathbf{w})p(\mathbf{W} = \mathbf{w})$.*

Proof. Assume $\mathbf{W} \cap \{\mathbf{V}, \mathbf{U}\} = \emptyset$. Furthermore, G, \hat{G} are again the original and intervened causal graph and $p = p_G$. Now, $p(\mathbf{V}_i = \mathbf{v}_i | do(\mathbf{U}_j = \mathbf{u}_j)) = p_{\hat{G}}(\mathbf{V}_i = \mathbf{v}_i | \mathbf{U}_j = \mathbf{u}_j)$

$$\begin{aligned}
 &= \sum_{\mathbf{w}} p_{\hat{G}}(\mathbf{V}_i = \mathbf{v}_i, \mathbf{W} = \mathbf{w} | \mathbf{U}_j = \mathbf{u}_j) \\
 &= \sum_{\mathbf{w}} p_{\hat{G}}(\mathbf{V}_i = \mathbf{v}_i | \mathbf{U}_j = \mathbf{u}_j, \mathbf{W} = \mathbf{w})p_{\hat{G}}(\mathbf{W} = \mathbf{w}) \\
 &= \sum_{\mathbf{w}} p(\mathbf{V}_i = \mathbf{v}_i | \mathbf{U}_j = \mathbf{u}_j, \mathbf{W} = \mathbf{w})p(\mathbf{W} = \mathbf{w}) .
 \end{aligned}$$

The first equality follows, by definition, from *do*-calculus as argued in Prop. 1, i.e., the intervention amounts to the observation in the intervened system. The second and third equality are transformations

according to the rules of probability theory: the second step follows the sum rule and the third step follows the chain rule. The last line follows from the assumptions of autonomy and invariance i.e., that interventions are local and invariant to whether they occur naturally or artificially. \square

The set of variables \mathbf{W} is called (*valid adjustment set*) (see Def. 6.38 [Peters et al., 2017]) if it adjusts the observational setting such that the causal effect captured by the intervention becomes *unconfounded*¹⁰. For the Causal Health SCM \mathfrak{C} which induces the simple causal graph $A \rightarrow F, \{A, F\} \rightarrow H, H \rightarrow M$, the equivalence of Props. 1 and 2 depends on the inference query. While an intervention on A is trivially unconfounded $p(H = h \mid do(A = a)) = p(H = h \mid A = a)$, an intervention on F would require adjustment via e.g. $\{A\}$, that is, $p(H = h \mid do(F = f)) = \sum_a p(H = h \mid F = f, A = a)p(A = a)$.

A.7 Example of an Analytical Derivation for ATE

Consider the non-confounding case of the ATE or causal effect of a Burglary (B) on an Alarm (A) (where Q is Earthquake) from the Earthquake data set. From the law of iterated expectations, it follows:

$$\begin{aligned} &ATE(\text{Treatment}=B, \text{Effect}=A) \\ &= \mathbb{E}[A \mid do(B = 1)] - \mathbb{E}[A \mid do(B = 0)] \\ &= \mathbb{E}_Q[\mathbb{E}[A \mid do(B = 1), Q] - \mathbb{E}[A \mid do(B = 0), Q]] \\ &= 0.99322 - 0.0598 = \mathbf{0.93342} \end{aligned}$$

with

$$\begin{aligned} &\mathbb{E}_Q[\mathbb{E}[A \mid do(B = 1), Q]] \\ &= \sum_e \mathbb{E}[A \mid do(B = 1), Q = e]p(Q = e) \\ &= \sum_e p(A = 1 \mid do(B = 1), Q = e)p(Q = e) \\ &= \sum_e p(A = 1 \mid B = 1, Q = e)p(Q = e) \\ &= 0.71 * 0.02 + 0.999 * 0.98 = 0.99322 \end{aligned}$$

and analogously for $\mathbb{E}_Q[\mathbb{E}[A \mid do(B = 0), Q]]$.

The ATE tells us that a burglary has a strong effect on the alarm to be triggered which is consistent with our human intuition as the alarm is specifically designed to trigger in an event of theft.

¹⁰Mathematically, the causal effect from X to Y is confounded if $p(Y \mid do(X)) \neq p(Y \mid X)$

A.8 Further Numerical Evaluation

More numerical evaluation, using Jensen-Shannon-Divergence as the discrepancy measure for the simulated ground truth distribution against the estimates of iSPN and the generative competition. A lower score suggests a better approximation. We consider a cycle permuted experimental setup in which each experiment considers a different uniform intervention of the currently selected variable of choice. Generally, iSPN outperforms the baselines in its estimate precision under fair (i.e., similar neural capacities, same amount of data passes, same amount of random seeds under consideration):

Method Query	iSPN	MADE	MDN	Method Query	iSPN	MADE	MDN
x-ray	0.002	1.262	0.398	Burglary	0.000	1.083	0.182
tub	0.009	0.004	0.176	Earthquake	0.000	0.005	0.465
lung	0.002	0.003	0.285	Alarm	0.001	0.048	0.312
either	0.009	0.022	0.089	MaryCalls	0.005	0.033	0.084
Method Query	iSPN	MADE	MDN	Method Query	iSPN	MADE	MDN
Smoker	0.003	0.002	0.064	Age	0.000	0.003	0.069
Pollution	0.005	0.385	0.305	Food Habits	0.013	0.037	0.108
Cancer	0.003	0.002	0.064	Health	0.006	0.007	0.073
Xray	0.001	0.305	0.066	Mobility	0.037	0.060	0.079

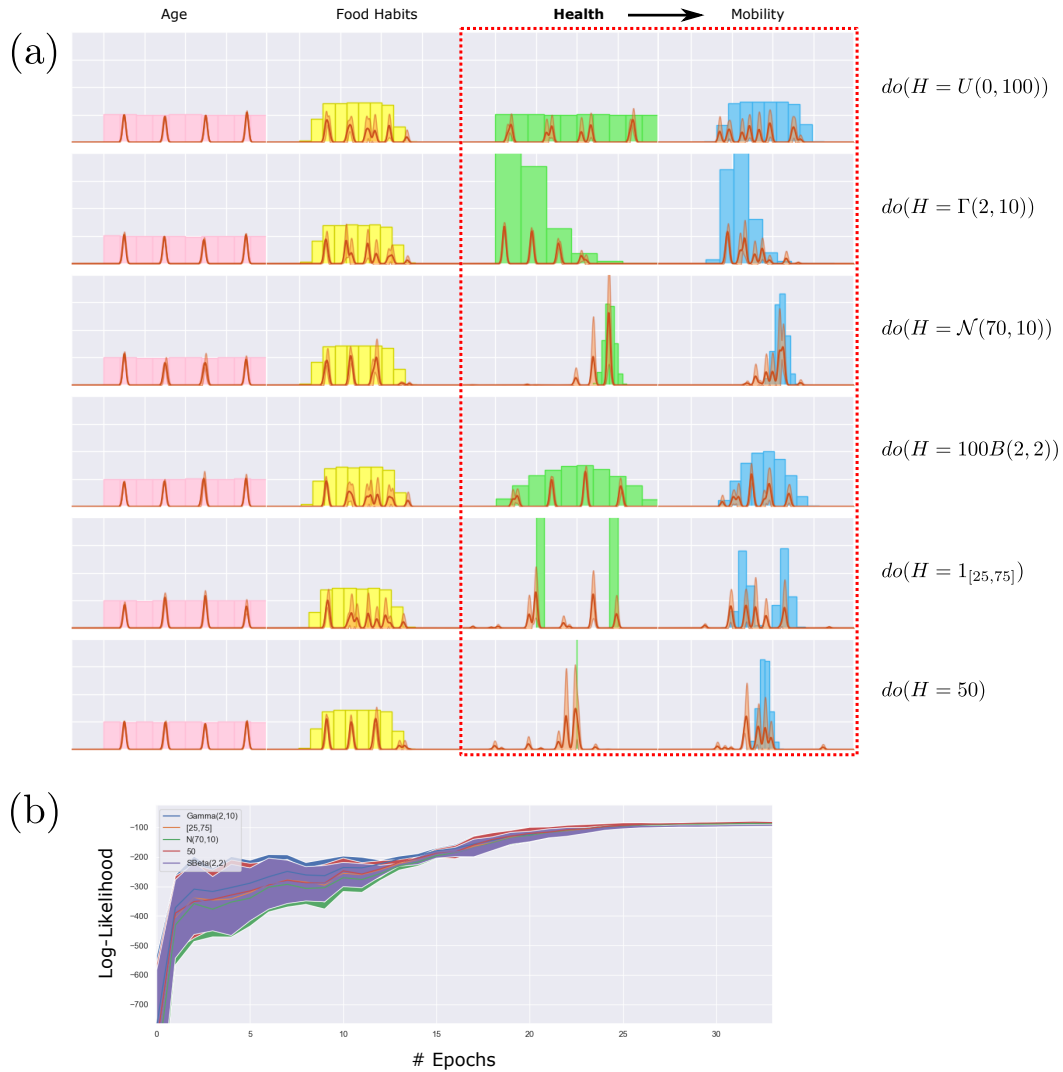


Figure 6: **Ablation Study on Different Intervention Types, Noise Terms and Instantiations.** Training results for different kinds of interventions on the continuous Causal Health data set are being presented, with (a) presenting the learned (mean) density functions for a given intervention on H , where we consider different noise distributions normal $\mathcal{N}(\mu, \sigma^2)$, Gamma $\Gamma(p, q)$, and Beta $B(a, b)$ but also different modifications, e.g. the non-standard Beta distribution $(k-l)B(a, b) + l$ and intervention types, e.g. perfect interventions $do(H = a)$, $a \in \mathbb{R}$. Below (b) shows the respective mean objective curves (log-likelihood), indicating consistent training and convergence on the continuous data set for all 3 seeds per configuration.



Figure 7: **Single Best Density vs Mean Density.** An example of the visual discrepancy between the performance of the single best seed and the mean performance across multiple seeds. As can be observed in the top row, the single best seed fits all the different marginal distributions accurately, while the mean performance of the given training setup and model architecture (presented in the bottom row) shows deviation especially on regions of low or none support i.e., consider $p(H \neq 50 | do(H = 50)) > 0$ that have more emphasized peaks although ideally none (or insignificant ones, considerably noise, as for the single best seed) should be observed.

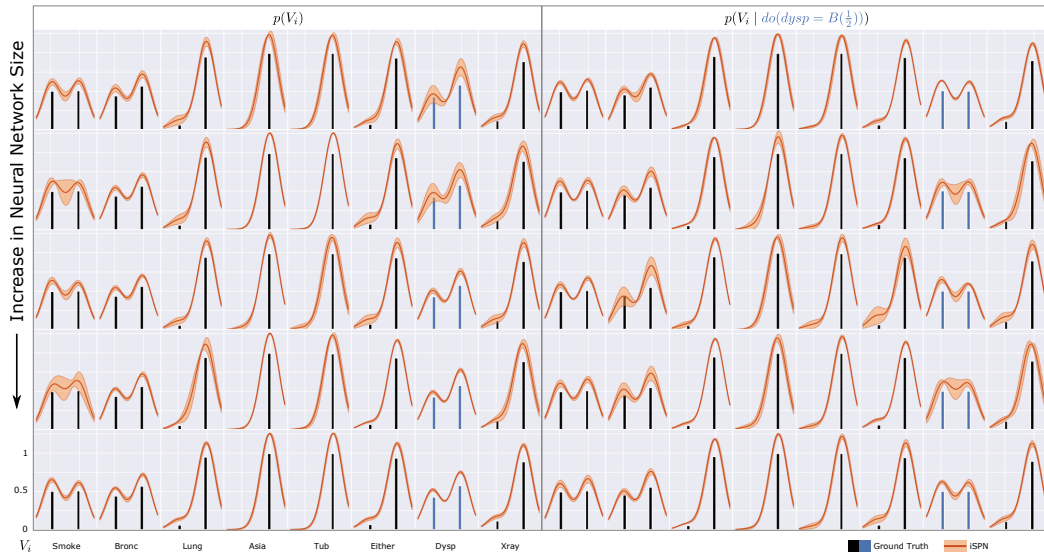


Figure 8: **Effect of size of neural network.** We test robustness of iSPN by training with neural networks of 5 different parameter sizes on the ASIA data set. Each row represents neural network size, the first 8 columns represent the observational distributions of 8 variables and the next 8 columns represent the learned marginal distributions upon intervention with $do(\cdot)$.

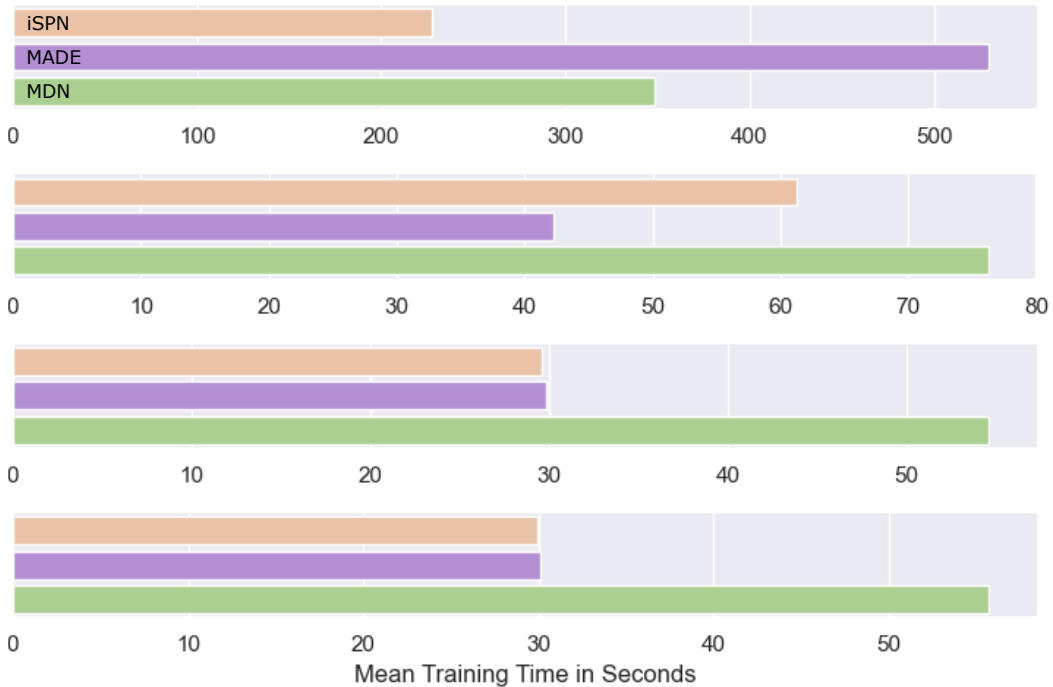


Figure 9: **Runtimes over different data sets.** From top to bottom, as in Fig.4: Causal Health (H), ASIA (A), Earthquake (E), Cancer (C). On the binary data sets (A, E, C), MADE due to its single-model form is able to match iSPN and slightly improve upon iSPN, however, for the hybrid-model real-world-esque (H) the speed advantage of the over-parameterized models and especially iSPN becomes apparent. Important: note the scales on H, iSPN significantly outperforms the other models.

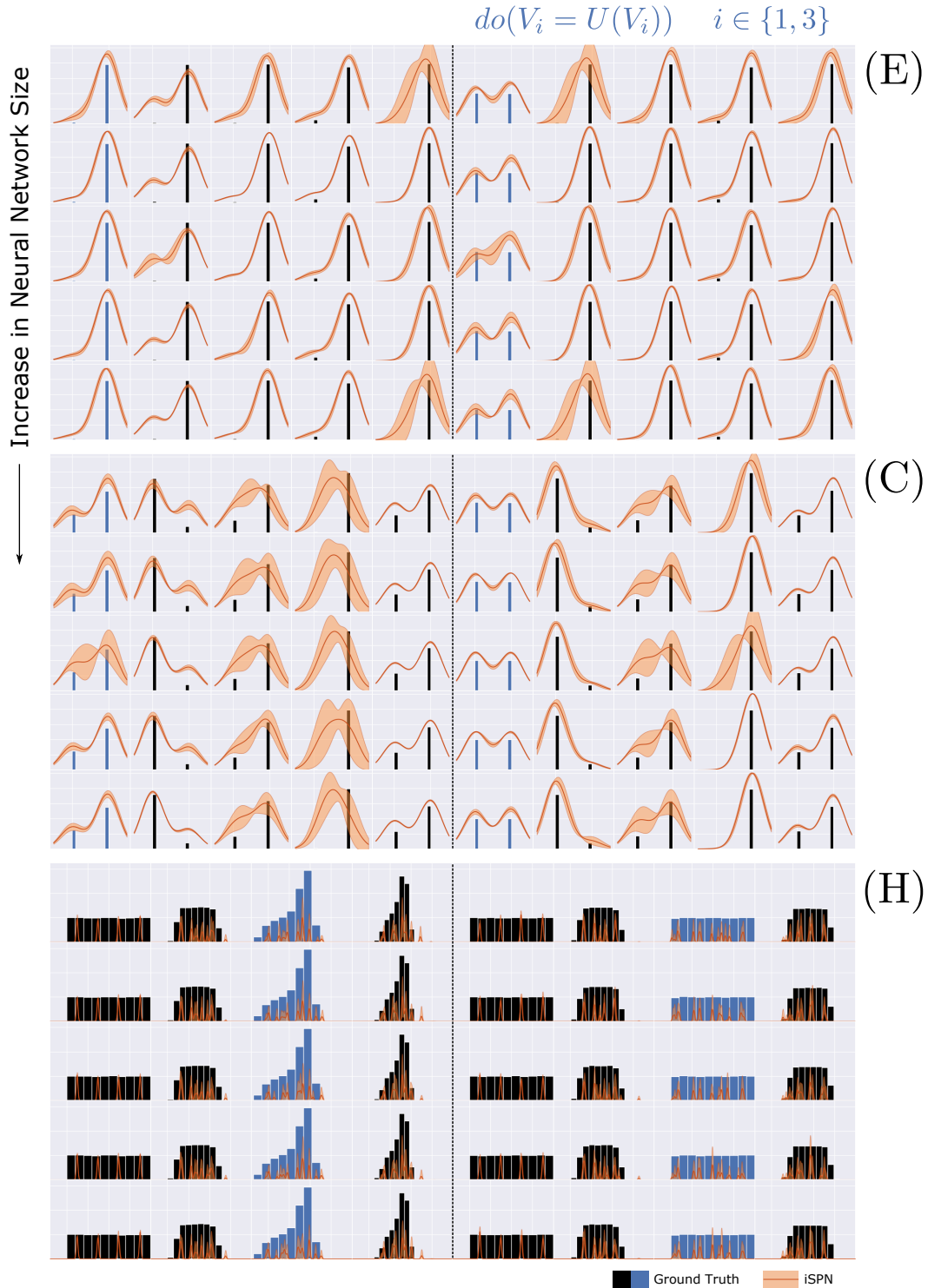


Figure 10: **Ablation Study on Influence of Neural Network Size.** A cohort of trained model configurations that only differ in the size of their respective function approximation modules (neural network) and their mean performances across the observational and one interventional setting (uniform intervention being Bernoulli $B(\frac{1}{2})$ for discrete and Uniform $U(V_i)$ for continuous variables) are being presented for the remaining data sets: Earthquake (E), Cancer (C), Causal Health (H). As can be observed, the mean performance stays mainly consistent across the different function approximation capacities while the variance can differ slightly.